Inorg. Chem. **2006**, *45*, 9789–9797

Electronic Structure and Excited States of Rhenium(I) Amido and Phosphido Carbonyl–Bipyridine Complexes Studied by Picosecond Time-Resolved IR Spectroscopy and DFT Calculations

Anders Gabrielsson,[†] Michael Busby,[†] Pavel Matousek,[‡] Michael Towrie,[‡] Eva Hevia,[§] Luciano Cuesta,[§] Julio Perez,[§] Stanislav Záliš,*[,£] and Antonín Vlček, Jr.*[,†,£]

School of Biological and Chemical Sciences, Queen Mary, University of London, Mile End Road, London E1 4NS, United Kingdom, Central Laser Facility, CCLRC Rutherford Appleton Laboratory, Chilton, Didcot, Oxfordshire OX11 0QX, United Kingdom, Departamento de Quimica Organica e Inorganica, Facultad de Quimica, Universidad de Oviedo, Oviedo 33006, Spain, and J. Heyrovský Institute of Physical Chemistry, Academy of Sciences of the Czech Republic, Dolejškova 3, CZ-182 23 Prague, Czech Republic

Received August 5, 2006

UV–vis absorption and picosecond time-resolved IR (TRIR) spectra of amido and phosphido complexes *fac*-[Re(ER$_2$)(CO)$_3$(bpy)] (ER$_2$ = NHPh, NTol$_2$, PPh$_2$, bpy = 2,2′-bipyridine, Tol = 4-methylphenyl) were investigated in conjunction with DFT and TD-DFT calculations in order to understand their ground-state electronic structure, low-lying electronic transitions and excited-state character and dynamics. The HOMO is localized at the amido/phosphido ligand. Amide and phosphide ligands are σ-bonded to Re, the π interaction being negligible. Absorption spectra show a weak band at low energies (1.7–2.1 eV) that arises from essentially pure ER$_2$ → bpy ligand-to-ligand charge transfer (LLCT). The lowest excited state is the corresponding triplet, ^{3}LLCT. Low triplet energies and large distortions diminish the excited-state lifetimes to 85 and 270 ps for NHPh and NTol$_2$, respectively, and to ca. 30 ps for PPh$_2$. ν(CO) vibrations undergo only very small ($\leq$10 cm^{-1}) shifts upon excitation, attesting to its LLCT character, which hardly affects the electron-density distribution on the Re(CO)$_3$ moiety. Relaxation of the ^{3}LLCT state occurs with complex dynamics ranging from units to tens of picoseconds. The "pure" LLCT excitation, which does not mix with the Re → bpy MLCT character, is a unique feature of the amido/phoshido complexes, whose lowest excited state can be viewed as containing a highly unusual aminyl/phosphinyl radical-cationic ligand. For comparison, the amino and phosphino complexes *fac*-[Re(NHPh$_2$)(CO)$_3$(bpy)]$^+$ and *fac*-[Re(PPh$_3$)(CO)$_3$(bpy)]$^+$ are shown to have the usual Re → bpy ^{3}MLCT lowest excited states, characterized by upshifted ν(CO) bands.

Introduction

Amido and phosphido complexes of low-valent transition metals show rather unusual chemical, structural, and spectroscopic properties that arise from the large electron density on the ligand. This is, for example, the case of the complexes[1] *fac*-[Re(ER$_2$)(CO)$_3$(bpy)] (E = N or P; R = Ph, Tol = 4-methylphenyl, or H), which are prone to an electrophilic attack at the N or P donor atom and undergo various insertion reactions.[1−5] Free rotation around the Re−N and Re−P bonds, observed by NMR, indicates the lack of metal−ligand π-bonding.[1] Amido complexes containing an NHAryl or NAryl$_2$ ligand show planar geometry at the N donor atom, which enters π interaction with only one aryl ring. The phosphido complex [Re(PPh$_2$)(CO)$_3$(bpy)] is pyramidal at the P atom, with rather long Re−P bonds.[1] The strongly

* To whom correspondence should be addressed. E-mail: a.vlcek@qmul.ac.uk (A.V.); zalis@jh-inst.cas.cz (S.Z.).
[†] University of London.
[‡] Rutherford Appleton Laboratory.
[§] Universidad de Oviedo.
[£] Academy of Sciences of the Czech Republic.

(1) Hevia, E.; Pérez, J.; Riera, V.; Miguel, D. *Organometallics* **2002**, *21*, 1966−1974.
(2) Hevia, E.; Pérez, J.; Riera, V.; Miguel, D. *Organometallics* **2003**, *22*, 257−263.
(3) Hevia, E.; Pérez, J.; Riera, V.; Miguel, D. *Chem. Commun.* **2002**, 1814−1815.
(4) Cuesta, L.; Hevia, E.; Morales, D.; Perez, J.; Riera, V.; Rodríguez, E.; Miguel, D. *Chem. Commun.* **2005**, 116−117.
(5) Cuesta, L.; Hevia, E.; Morales, D.; Perez, J.; Riera, V.; Seitz, M.; Miguel, D. *Organometallics* **2005**, *24*, 1772−1775.

10.1021/ic0614768 CCC: $33.50
Published on Web 11/01/2006

electron-donating character of the amido and phosphido ligands in these complexes is manifested by low CO stretching frequencies.[1]

The large electron density on the nitrogen or phosphorus donor atom is also expected to affect the nature of low-lying electronic transitions and excited states. This is already manifested by the colors: While most Re(I) carbonyl−bipyridine complexes are yellow, the amides are green and the PPh_2 complex is dark blue. Amido and phosphido complexes, *fac*-[Re(ER_2)$(CO)_3$(bpy)], thus offer a unique opportunity to unravel the effects of very electron-rich ligands on electronic transitions and excited-state behavior of Re(I) carbonyl−bipyridine complexes. With this aim, we have investigated the UV−vis absorption spectra and picosecond time-resolved infrared (TRIR) spectra of the complexes *fac*-[Re(ER_2)$(CO)_3$(bpy)] (ER_2 = NHPh, $NTol_2$, PPh_2). The experimental results are complemented by DFT and TD-DFT calculations, which show the electron-density redistribution upon excitation, allowing us to assess the excited-state character. It is shown that the presence of an amido/phosphido ligand gives rise to a low-lying $ER_2 \rightarrow$ bpy ligand-to-ligand charge transfer (LLCT) excited state, whereby the ER_2 ligand is oxidized to a highly unusual[6] coordinated aminyl or phosphinyl radical cation $ER_2^{+\bullet}$. To our surprise, the detailed nature and, hence, photophysics of this state is very different from the mixed MLCT/LLCT states of analogous Re^I complexes with π-donating ligands, such as halides or NCS^-.[7−12]

Experimental Section

The complexes *fac*-[Re(ER_2)$(CO)_3$(bpy)] (ER_2= NHPh, NPh_2, $NTol_2$, NHTol, PPh_2) and *fac*-[Re(PPh_3)$(CO)_3$(bpy)]BAr'_4 (BAr'_4 = B(3,5-bis(trifluoromethyl)phenyl)$_4$) were prepared using the procedures described previously.[1, 13]

The new complex [Re($HNPh_2$)$(CO)_3$(bipy)]BAr'_4 was synthesized as follows. Dichloromethane (15 mL) was added to a mixture of [Re(OTf)$(CO)_3$(bipy)] (OTf = SO_3CF_3)[14] (0.050 g, 0.086 mmol) and $NaBAr'_4$ (0.077 g, 0.086 mmol). After 15 min of stirring, diphenylamine (0.015 g, 0.088 mmol) was added, and the resulting solution was stirred 10 min and then filtered with a cannula tipped with filter paper. Slow diffusion of hexane into this solution at −20 °C afforded yellow crystals. Yield: 0.041 g, 78%. IR (CH_2Cl_2): 2041s, 1935s, br. ^{1}H NMR (CD_2Cl_2): 9.01 [m, 2H, bipy], 8.70 [m, 2H, Ph], 8.14 [m, 4H, bipy], 7.77 [8H, H_{ortho} BAr'_4], 7.58 [m, 6H, 4H of H_{para} BAr'_4 and 2H of bipy], 7.23 [m, 4H, Ph], 7.01 [m, 4H, Ph], 5.16 [s broad, 1H, NH]. ^{13}C{^{1}H}NMR: 197.7 [2 CO], 195.3 [CO], 162.2 [q (49.8 Hz), C_i BAr'_4], 156.1, 155.7, [bipy], 148.13 [Ph], 143.2 [bipy], 135.2 [s, C_o BAr'_4], 132.6 [bipy], 131.5 [Ph], 128.2 [q (31.1 Hz), C_m BAr'_4], 128.8, 126.4 [Ph], 125.0 [q (272.6 Hz), CF_3], 123.7 [bipy], 117.9 [C_p BAr'_4]. Anal. Calcd for $C_{57}H_{31}BF_{24}N_3O_3Re$: C, 46.93, H, 2.14, N, 2.88. Found: C, 47.08, H, 2.19, N, 2.77.

Stationary FTIR and UV−vis absorption spectra were obtained using Perkin-Elmer PE1720X and HP8453 spectrometers, respectively. NMR spectra were measured on a Bruker AC300 instrument. The amido and phosphido complexes were characterized and their purity checked by comparison of their FTIR and ^{1}H NMR spectra with those reported[1] previously. All spectroscopic studies were performed in solvents of a spectroscopic quality (Aldrich), which were degassed by bubbling with argon or using standard Schlenk techniques. IR cells for TRIR measurements were filled with the sample solution under the flow of nitrogen in an Aldrich AtmosBag. Because of oxygen- and moisture-sensitivity of the samples, the solutions were not flowed through the IR cells.

TRIR spectra were obtained using the equipment and procedures described previously.[15−17] In short, the sample solution was excited (pumped) at 400 nm, using frequency-doubled pulses from a Ti:sapphire laser of ∼150 fs duration (fwhm), 4−5 μJ per pulse. TRIR spectra were probed at selected time delays with IR (∼150 fs) pulses obtained by difference-frequency generation. The IR probe pulses cover spectral range ca. 200 cm^{-1} wide and are tunable from 1000 to 5000 cm^{-1}. The diameter of the pump and probe laser pulses was 150−200 μm. The spectra were investigated only in the region of ν(CO) vibrations. The measurements were performed on static sample solutions in a CaF_2 IR cell, which was raster-scanned to prevent localized laser-heating and photochemical decomposition. The cell thickness of 0.1−0.135 mm was used for THF solutions. All spectral and kinetic fitting was performed using Microcal Origin 7 software.

Quantum Chemical Calculations. The electronic structures of the complexes *fac*-[Re(ER_2)$(CO)_3$(bpy)] were calculated by DFT methods using the Gaussian03[18] program package. Calculations employed the hybrid functionals B3LYP[19] or Perdew, Burke, Ernzerhof[20,21] exchange and correlation functional (PBE0). The

(6) Büttner, T.; Geier, J.; Frison, G.; Harmer, J.; Calle, C.; Schweiger, A.; Schönberg, H.; Grützmacher, H. *Science* **2005**, *307*, 235−238.
(7) Stufkens, D. J.; Vlček, A., Jr. *Coord. Chem. Rev.* **1998**, *177*, 127−179.
(8) Vlček, A., Jr.; Záliš, S. *Coord. Chem. Rev.* **2006**, *250*, in press.
(9) Stufkens, D. J. *Comments Inorg. Chem.* **1992**, *13* (6), 359−385.
(10) Blanco-Rodríguez, A. M.; Gabrielsson, A.; Motevalli, M.; Matousek, P.; Towrie, M.; Šebera, J.; Záliš, S.; Vlček, A., Jr. *J. Phys. Chem. A* **2005**, *109*, 5016−5025.
(11) Stor, G. J.; Stufkens, D. J.; Oskam, A. *Inorg. Chem.* **1992**, *31*, 1318−1319.
(12) Rossenaar, B. D.; Stufkens, D. J.; Vlček, A., Jr. *Inorg. Chem.* **1996**, *35*, 2902−2909.
(13) Hevia, E.; Pérez, J.; Riera, V.; Miguel, D.; Kassel, S.; Rheingold, A. *Inorg. Chem.* **2002**, *41*, 4673−4679.
(14) Hino, J. K.; Della Ciana, L.; Dressick, W. J.; Sullivan, B. P. *Inorg. Chem.* **1992**, *31*, 1072−1080.
(15) Liard, D. J.; Busby, M.; Farrell, I. R.; Matousek, P.; Towrie, M.; Vlček, A., Jr. *J. Phys. Chem. A* **2004**, *108*, 556−567.
(16) Vlček, A., Jr.; Farrell, I. R.; Liard, D. J.; Matousek, P.; Towrie, M.; Parker, A. W.; Grills, D. C.; George, M. W. *J. Chem. Soc., Dalton Trans.* **2002**, 701−712.
(17) Towrie, M.; Grills, D. C.; Dyer, J.; Weinstein, J. A.; Matousek, P.; Barton, R.; Bailey, P. D.; Subramaniam, N.; Kwok, W. M.; Ma, C. S.; Phillips, D.; Parker, A. W.; George, M. W. *Appl. Spectrosc.* **2003**, *57*, 367−380.
(18) Frisch, M. J.; Trucks, G. W.; Schlegel, H. B.; Scuseria, G. E.; Robb, M. A.; Cheeseman, J. R.; Montgomery, J. A., Jr.; Vreven, T.; Kudin, K. N.; Burant, J. C.; Millam, J. M.; Iyengar, S. S.; Tomasi, J.; Barone, V.; Mennucci, B.; Cossi, M.; Scalmani, G.; Rega, N.; Petersson, G. A.; Nakatsuji, H.; Hada, M.; Ehara, M.; Toyota, K.; Fukuda, R.; Hasegawa, J.; Ishida, M.; Nakajima, T.; Honda, Y.; Kitao, O.; Nakai, H.; Klene, M.; Li, X.; Knox, J. E.; Hratchian, H. P.; Cross, J. B.; Bakken, V.; Adamo, C.; Jaramillo, J.; Gomperts, R.; Stratmann, R. E.; Yazyev, O.; Austin, A. J.; Cammi, R.; Pomelli, C.; Ochterski, J. W.; Ayala, P. Y.; Morokuma, K.; Voth, G. A.; Salvador, P.; Dannenberg, J. J.; Zakrzewski, V. G.; Dapprich, S.; Daniels, A. D.; Strain, M. C.; Farkas, O.; Malick, D. K.; Rabuck, A. D.; Raghavachari, K.; Foresman, J. B.; Ortiz, J. V.; Cui, Q.; Baboul, A. G.; Clifford, S.; Cioslowski, J.; Stefanov, B. B.; Liu, G.; Liashenko, A.; Piskorz, P.; Komaromi, I.; Martin, R. L.; Fox, D. J.; Keith, T.; Al-Laham, M. A.; Peng, C. Y.; Nanayakkara, A.; Challacombe, M.; Gill, P. M. W.; Johnson, B.; Chen, W.; Wong, M. W.; Gonzalez, C.; Pople, J. A. *Gaussian 03*, revision C.02; Gaussian, Inc.: Wallingford, CT, 2004.
(19) Becke, A. D. *J. Chem. Phys.* **1993**, *98*, 5648.
(20) Perdew, J. P.; Burke, K.; Ernzerhof, M. *Phys. Rev. Lett.* **1996**, *77*, 3865.
(21) Adamo, C.; Barone, V. *J. Chem. Phys.* **1999**, *110*, 6158−6170.

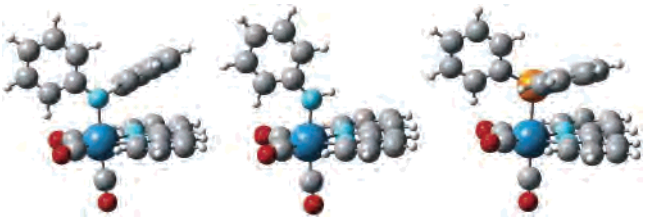

Figure 1. DFT-calculated structures of *fac*-[Re(NPh_2)($CO)_3$(bpy)] (left), *fac*-[Re(NHPh)($CO)_3$(bpy)] (middle), and *fac*-[Re(PPh_2)($CO)_3$(bpy)] (right). The prefix "*fac*-" will be hereafter omitted.

solvent was described by CPCM.[22] Low-lying singlet and triplet excited states at the ground-state geometry were calculated by TD-DFT. Optimized excited-state geometry was calculated for the lowest triplet state of each complex by the unrestricted Kohn−Sham approach (UKS). Calculations of the vibrational frequencies were performed at these optimized geometries. The difference density plots were drawn using the GaussView software. UV−vis absorption spectra were simulated with the GaussSum[23] software, including all calculated transitions. Gaussian shapes (3000 cm^{-1} fwhm) of the absorption bands were assumed.

For H, C, N, O, and P atoms, either 6-31G* polarized double-ζ basis sets[24] (geometry optimization and vibrational analysis) or cc-pvdz correlation consistent polarized valence double-ζ basis sets[25] (TD-DFT) were used. The Re atom was described by quasirelativistic effective core pseudopotentials and corresponding optimized set of basis functions.[26]

Results

Ground-State Molecular and Electronic Structures. Experimental X-ray structures were reported earlier[1] for [Re(NHPh)($CO)_3$(bpy)], [Re(NPh_2)($CO)_3$(bpy)], and [Re(PPh_2)-($CO)_3$(bpy)]. DFT calculations (B3LYP) well reproduce their salient features, Figure 1. In particular, the geometry around the N atom of the amido ligand is planar, indicating a (formally) sp^2 configuration. The two Ph rings of NPh_2 are orthogonal. In contrast, the geometry of the P atom was both measured and calculated to be pyramidal (sp^3).

Calculated bond distances and angles agree reasonably well with the experimental ones, see Table S1. Quantitatively, all the Re−ligand bonds are slightly longer than those determined from the crystal structures. The nonequivalence of the two N−C(Ph) bonds observed for NPh_2 is well reproduced computationally, although the calculated bond-length difference is smaller. It is possible that the minor differences between calculated and measured bonding parameters originate in crystal lattice effects. For example, the crystal structures show large differences between the two equatorial Re−C(O) and Re−N(bpy) bonds and the two phenyl rings of the PPh_2 or NPh_2 ligands, while free rotation occurs[1] in the solution. In fact, DFT indicates that several conformers of a similar energy can be present in the solution, see Figure S1. The results reported hereinafter were obtained for the most stable conformers.

(22) Cossi, M.; Rega, N.; Scalmani, G.; Barone, V. *J. Comput. Chem.* **2003**, *24*, 669.
(23) O'Boyle, N. M.; Vos, J. G. *GaussSum 0.8*; Dublin City University: 2004.
(24) Hariharan, P. C.; Pople, J. A. *Theor. Chim. Acta* **1973**, *28*, 213.
(25) Woon, D. E.; Dunning, T. H., Jr. *J. Chem. Phys.* **1993**, *98*, 1358.
(26) Andrae, D.; Häussermann, U.; Dolg, M.; Stoll, H.; Preuss, H. *Theor. Chim. Acta* **1990**, *77*, 123−141.

Table 1. DFT PBE0/CPCM-THF Calculated One-Electron Energies and Compositions of Selected Highest Occupied and Lowest Unoccupied Molecular Orbitals of [Re($NTol_2$)($CO)_3$(bpy)] Expressed in Terms of Composing Fragments

MO	*E* (eV)	prevailing character	Re	CO_{ax}	CO_{eq}	N	Tol_2	bpy
			Unoccupied					
126a	−0.69	Re+CO	26	12	52	1	3	5
125a	−1.23	π* bpy	1	0	2	0	0	96
124a	−1.45	π* bpy	1	0	2	0	1	95
123a	−2.40	π* bpy	2	0	3	1	0	94
			Occupied					
122a	−4.53	$NTol_2$	5	3	2	36	52	1
121a	−6.26	$NTol_2$	10	3	1	5	81	1
120a	−6.47	Re	47	11	10	0	26	5
119a	−6.58	$NTol_2$	35	6	9	0	44	5
118a	−6.62	Re	22	4	7	0	64	3
117a	−6.82	Re	65	2	29	0	1	3
116a	−6.93	$NTol_2$	1	0	0	0	96	3
115a	−7.52	π bpy	0	0	0	0	2	97

Table 2. DFT PBE0/CPCM-THF Calculated One-Electron Energies and Compositions of Selected Highest Occupied and Lowest Unoccupied Molecular Orbitals of [Re(PPh_2)($CO)_3$(bpy)] Expressed in Terms of Composing Fragments

MO	*E* (eV)	prevailing character	Re	CO_{ax}	CO_{eq}	P	Ph_2	bpy
			Unoccupied					
122a	−0.73	Re+CO	27	18	45	2	3	4
121a	−1.09	π* bpy	1	0	2	0	1	95
120a	−1.23	π* bpy	1	1	1	1	0	95
119a	−2.24	π* bpy	2	1	2	2	1	92
			Occupied					
118a	−4.95	PPh_2	13	4	1	51	28	3
117a	−6.40	Re	50	11	10	5	19	5
116a	−6.55	Re	52	10	11	1	18	8
115a	−6.71	Re	65	1	28	0	5	2
114a	−6.79	PPh_2	6	1	2	1	89	1
113a	−6.84	PPh_2	11	2	3	3	75	5
110a	−7.42	π bpy	2	0	1	3	13	81

Ground-state electronic structures can be qualitatively understood from the characters of the high-lying Kohn−Sham occupied molecular orbitals, see Tables 1 and 2 and Figure 2. The HOMO of [Re($NTol_2$)($CO)_3$(bpy)] is essentially a π* orbital of the amide. It is localized predominantly on the N atom and on the π-conjugated aryl ring, which is perpendicular to the Re($CO)_2$(bpy) plane, see Figure 2. The HOMO is π-antibonding with respect to one N−C(aryl) bond. It is Re−N π-nonbonding, since there is no corresponding Re dπ contribution. The HOMO−1 is also an amide π* orbital, localized mostly on the other aryl ring, Figure 2. Other high-lying occupied MOs consist mostly of π-bonding orbitals of the π-conjugated aryl ring and π orbitals of the $Re(CO)_3$ unit, with a significant Re dπ component. The participation of the N donor atom being negligible, they are π-nonbonding toward the Re−N bond. The first three unoccupied orbitals are predominantly of a π* bpy character, like in all other Re(I) carbonyl−bipyridine complexes.

The pyramidal configuration of the phosphido ligand makes the HOMO of [Re(PPh_2)($CO)_3$(bpy)] essentially a P-localized lone electron pair, which partly interacts with a Re dπ orbital, Figure 2. The HOMO−1 and HOMO−2 are highly mixed, but Re−P π nonbonding. HOMO−3 is a Re-

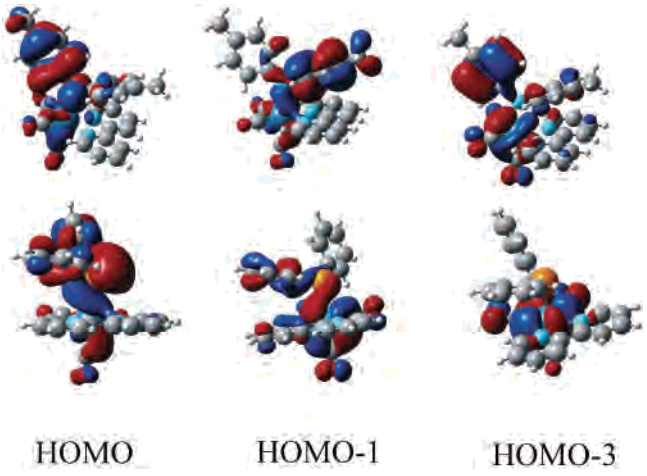

Figure 2. Spectroscopically relevant KS molecular orbitals of [Re($NTol_2$)-($CO)_3$(bpy)] (top) and [Re(PPh_2)($CO)_3$(bpy)] (bottom). Calculated by PBE0/CPCM-THF.

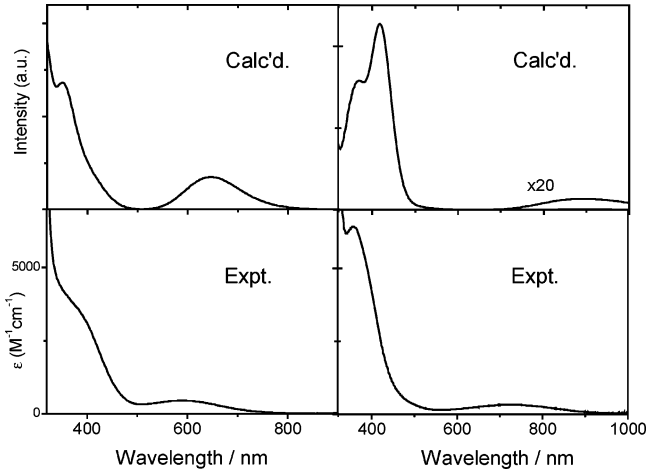

Figure 3. UV−vis spectra of [Re(PPh_2)($CO)_3$(bpy)] (left) and [Re($NTol_2$)-($CO)_3$(bpy)] (right). Bottom: experimental spectra in THF. Top: Simulated spectra based on TD-DFT/PBE0/CPCM-THF calculations; 0.4 eV fwhm assumed. Top-right: High-energy transitions were not included in the simulation. Intensity of the simulated lowest band is multiplied by the factor of 20.

based MO, localized in the Re($CO)_2$(bpy) plane. The first three unoccupied orbitals again consist mostly of a π^*(bpy) character.

In conclusion, amido and phosphido ligands behave in Re(I) complexes as formal two-electron donors, bound by a single σ bond. There is no significant Re−N/P π interaction in the high-lying occupied MOs. The HOMO proper is localized on the amide/phosphide and occurs at rather high energies, with a large energy separation from the HOMO−1 and other occupied orbitals. This bonding pattern is different from that in analogous Re(I) complexes with π-donating ligands, such as halides or NCS^-, whose high-lying MOs are π-antibonding and π-bonding with respect to the Re−ligand bond, the HOMO and HOMO−1 forming a close-lying symmetry-related pair of orbitals.[8,10,27]

UV−Vis Absorption Spectra. Spectra of [Re($NTol_2$)-($CO)_3$(bpy)] and [Re(PPh_2)($CO)_3$(bpy)] measured in THF are shown in Figure 3, together with those calculated by TD-DFT. They exhibit a weak, broad band in the visible region (590−720 nm) that is unique for the [Re(ER_2)($CO)_3$(bpy)] complexes. TD-DFT calculations (Tables 3 and 4) show that this low-energy band arises almost exclusively from HOMO → LUMO excitation. Given the character of these orbitals, the corresponding transition can be described as ER_2 → bpy LLCT. It involves transfer of electron density from the amido N atom and the π-conjugated aryl of NR_2 or the phosphorus lone electron pair of PPh_2, whose phenyl rings are depopulated less. The ^{1}LLCT assignment of the lowest $a^1A \rightarrow b^1A$ transition is corroborated by calculated accompanying changes of the Mulliken populations, Table S6. For example, the $NTol_2$ ligand is depopulated by 0.84 e^- while the electron density on bpy increases by 0.92 e^-. The calculated charge separation is a little less for PPh_2, which is depopulated by 0.72 e^-.

Out of the higher electronic transitions of [Re($NTol_2$)-($CO)_3$(bpy)], which give rise to the group of intense bands below 500 nm, it is worth mentioning e^1A, f^1A, and h^1A. The transition to the e^1A state involves predominantly a $NTol_2$ → CO LLCT. Depopulation of the unconjugated aryl ring gives rise to the f^1A transition which thus has a $NTol_2$ → bpy LLCT character. The h^1A is a highly mixed transition which contains a 69% contribution from Re,$NTol_2$ → bpy MLCT/LLCT, where the electron density is excited from the Re dπ orbitals and the conjugated tolyl ring of the amido ligand. For [Re(PPh_2)($CO)_3$(bpy)], the high-energy absorption arises from a group of closely spaced LLCT transitions to higher unoccupied bpy-based orbitals, followed by f^1A PPh_2 → CO LLCT and a predominantly MLCT transition to h^1A.

The UV−vis spectrum of [Re(NHTol)($CO)_3$(bpy)] in CH_3-CN (Table S2) is very similar to that of [Re($NTol_2$)($CO)_3$-(bpy)]. The lowest NHTol → bpy LLCT band occurs at 2.00 eV, that is, 620 nm ($\epsilon \cong 280$ M^{-1} cm^{-1}). It was calculated by TD-DFT at 1.42 eV, corresponding to 99% HOMO → LUMO excitation, that is, NHTol → bpy LLCT.

In conclusion, the UV−vis absorption spectra show that the presence of a low-energy LLCT excited state is the salient feature of the amido/phosphido Re(I) carbonyl−diimine complexes. This state is inherently different from mixed LLCT/MLCT excited states which occur in halide or NCS− Re(I) complexes, since the depopulated MO is predominantly ER_2-localized instead of Re−L π-antibonding.

TRIR Spectra. TRIR spectra were studied in the region of ν(CO) vibrations with the aim to characterize the lowest ^{3}LLCT excited state and to determine its lifetime and relaxation dynamics. The spectra are presented in a difference mode, whereby the spectrum before excitation is subtracted from that measured at a given time delay after excitation. Positive bands thus correspond to photogenerated transients while the negative bands mirror the ground-state IR spectrum.

TRIR spectra of the amido complexes measured in THF are shown in Figures 4 and 5. The wavenumbers are summarized in Table 5. From the earliest time delays investigated (2−3 ps), the spectra show negative bleach bands due to the depleted ground-state population and broad transient features which occur at wavenumbers very similar to those of the ground-state bands. In particular, the two low-

(27) Vlček, A., Jr.; Záliš, S. *J. Phys. Chem. A* **2005**, *109*, 2991−2992.

Table 3. TD-DFT (PBE0/CPCM-THF) Calculated Singlet Excitation Energies (eV) for [Re(NTol$_2$)(Co)$_3$(bpy)] with Oscillator Strength Larger than 0.001, Calculated for THF Solution

state	main contributing excitations (%)	transition energy eV (nm)	osc. str.	expt eV (nm)	molar absorption M^{-1} cm^{-1}
b^1A	99(HOMO → LUMO)	1.42 (873)	0.001	1.71 (723)	330
c^1A	99(HOMO → LUMO+1)	2.38 (520)	0.001		
e^1A	94(HOMO → LUMO+3)	2.98 (416)	0.094		
f^1A	96(HOMO−1 → LUMO)	3.01 (411)	0.028	3.47 (357)	6520
h^1A	69(HOMO−3 → LUMO)	3.27 (379)	0.037		
i^1A	89(HOMO−5 → LUMO)	3.42 (361)	0.030		
	mixed ($\pi \rightarrow \pi^*$), bpy	4.34 (285)	0.165	4.32 (287)	29 620

Table 4. TD-DFT (PBE0/CPCM-THF) Singlet Excitation Energies (eV) for [Re(PPh$_2$)(Co)$_3$(bpy)] with Oscillator Strength Larger than 0.001, Calculated for THF Solution

state	main contributing excitations (%)	transition energy eV (nm)	osc. str.	expt eV (nm)	molar absorption M^{-1} cm^{-1}
b^1A	99(HOMO → LUMO)	1.92 (646)	0.048	2.10 (590)	454
c^1A	99 (HOMO → LUMO+1)	2.89 (429)	0.016		
d^1A	94(HOMO → LUMO+2)	3.04 (407)	0.019		
e^1A	97(HOMO−1 → LUMO)	3.15 (394)	0.022		
f^1A	94(HOMO → LUMO+3)	3.29 (377)	0.021	3.35 (370)[a]	3840
h^1A	76 (HOMO−3 → LUMO)	3.37 (367)	0.040		
i^1A	84(HOMO → LUMO+4)	3.56 (347)	0.132		
	mixed ($\pi \rightarrow \pi^*$), bpy	4.40 (282)	0.141	4.59 (270)	18700

[a] Broad shoulder starting at ca. 470 nm.

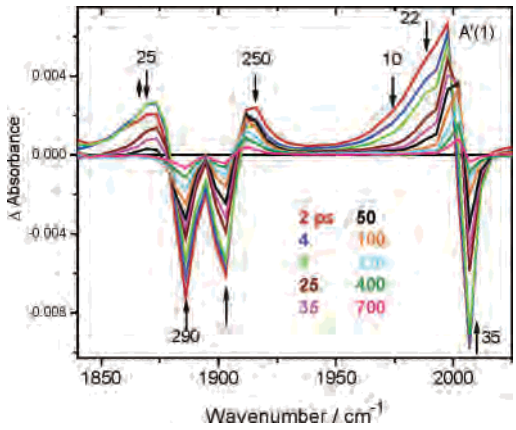

Figure 4. Difference TRIR spectra of [Re(NTol$_2$)(CO)$_3$(bpy)] in THF measured at selected time delays (in ps) after 400 nm excitation. Experimental points are separated by 4−5 cm^{-1}. The spectrum evolves in the direction of the arrows. The attached numbers show the corresponding decay lifetimes in ps.

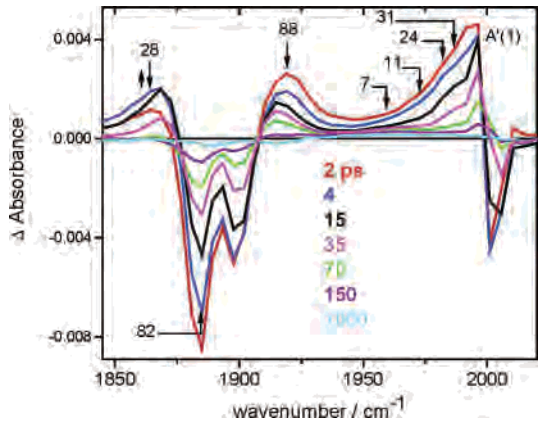

Figure 5. Difference TRIR spectra of [Re(NHPh)(CO)$_3$(bpy)] in THF measured at selected time delays (in ps) after 400 nm excitation. Experimental points are separated by 4−5 cm^{-1}. The spectrum evolves in the direction of the arrows. The attached numbers show the corresponding decay lifetimes in picoseconds.

frequency ground-state bands overlap with a broad transient feature that spans from about 1860 to 1920 cm^{-1}. The high-frequency band at about 2005 cm^{-1}, which is due to the A′-(1) vibration, shifts slightly lower upon excitation. The very small magnitude of the shift of the ν(CO) frequencies shows that the electron density distribution on the Re(CO)$_3$ unit hardly changes upon excitation, in agreement with the presumed NR_2 → bpy LLCT character of the excited state.

The excited-state A′(1) band has a shoulder at its low-energy side, ca. 10−15 cm^{-1} below the main maximum. It is especially prominent at short time delays. This shoulder is attributed to a "hot" $\upsilon = 1 \rightarrow 2$ transition from the first to the second A′(1) ν(CO) vibrational level of the ^{3}LLCT state. Its frequency is slightly lower than that of the $\upsilon = 0 \rightarrow 1$ transition due to anharmonicity.

TRIR spectra also point to an intriguing dynamics of the excited-state evolution. First, there is a drop in intensity between 2 and 6 ps above ca. 1900 cm^{-1} while the lowest band at 1860−75 cm^{-1} slightly rises in intensity until about 8 ps. Then, the excited-state spectral pattern shifts to higher wavenumbers and decays concomitantly. All these processes result in a pronounced dependence of the decay kinetics on the IR probe wavenumber. (Decay lifetimes measured at selected probe wavenumbers are shown in Figures 4 and 5.) Note that the decay kinetics measured in the region of the A′(1) excited-state maximum and the corresponding bleach (∼35 ps for NTol$_2$ and 30−50 ps for NHPh) result mostly from the dynamic shift of the excited-state band, which increasingly cancels out with the negative bleach band.

The TRIR spectra show that the lowest triplet state is populated during the first 2 ps after excitation. The presence

Table 5. Experimental and Calculated (B3LYP/CPCM-THF) ν(CO) Vibrational Wavenumbers of [Re(ER_2)($CO)_3$(bpy)][a]

[Re(NHPh)($CO)_3$(bpy)]				[Re($NTol_2$)($CO)_3$(bpy)]				[Re(PPh_2)($CO)_3$(bpy)]			
GS		ES		GS		ES		GS		ES	
calcd	exptl	calcd	exptl	calcd	exptl	calcd	exptl	calcd	exptl	calcd	exptl[b]
1883	1887	1898	1870−1920	1886	1887	1890	1873−1910	1893	1900	1901	1880−1930
1897	1897	1915		1901	1902	1904		1902	1900	1918	
2009	2002	2005	∼1998	2011	2007	2003	2001	2004	2000	2015	∼1991

[a] Experimental data were obtained from THF solutions. The lowest triplet excited state (ES) was calculated by UKS. All calculated values are scaled by a factor of 0.980. [b] Determined from the spectrum measured at 60 ps. Experimental values could be slightly underestimated because of incomplete excited-state relaxation.

of the low-frequency shoulder on the A′(1) band suggest that higher quanta of ν(CO) vibrations are populated initially and that this vibrational excitation persists for a few tens of picoseconds. The earliest spectral changes (2−6 ps) are hard to interpret, especially the rise of the lowest transient band. They could result either from the last stages of the population of the lowest triplet state from upper states or, more likely, from intramolecular vibrational energy redistribution (IVR) to the $\upsilon = 0,1$ ν(CO) levels which absorb more strongly in the IR than higher levels. The increase of the decay lifetime across the excited-state A′(1) band and its upward shift manifest the vibrational relaxation of higher ν(CO) levels, cooling of low-frequency vibrations, which are anharmonically coupled to ν(CO), and relaxation of the solvent.[28,29] Conversion between various excited-state conformers can contribute as well. All these relaxation processes are convoluted with the excited-state decay. The excited-state lifetime can be estimated from the decay at the high-energy sides of transient bands or by bleach recovery in those spectral regions where bleach and transient bands do not overlap. Values of 270 ± 44 and 85 ± 7 ps are estimated for [Re($NTol_2$)($CO)_3$(bpy)] and [Re(NHPh)($CO)_3$(bpy)], respectively, see Figures 4 and 5.

TRIR spectra of [Re(PPh_2)($CO)_3$(bpy)] are shown in Figure 6, and the ν(CO) wavenumbers are summarized in Table 5. Excited-state bands are shifted downward from their ground-state positions by some 9 cm^{-1}, indicating a PPh_2 → bpy LLCT character of the lowest triplet state. The spectra show only very small time-dependent shifts that would indicate the occurrence of relaxation processes. This could be caused by the broadness of the excited-state ν(CO) bands and the very fast decay that is comparable with or faster than relaxation. If this explanation is correct, then the excited-state ν(CO) wavenumbers listed in Table 5 could be slightly lower than those of a fully relaxed state. The large width of excited-state bands could be caused by the presence of several excited conformers, see Figure S2. The excited state decays completely in 100 ps, with a lifetime roughly estimated as 30 ps. The bleach bands decay concomitantly. The broad residual absorption between 1940 and 1990 cm^{-1}, which remains after the excited-state had decayed (at 100 ps), is most probably due to an impurity formed during the measurement by reaction with traces of oxygen or moisture. The presence of a small amount of impurity is evidenced by the weak bleach band at ∼1918 cm^{-1} observed in the 100 ps spectrum (Figure 6), which does not occur in the ground-state IR spectrum of [Re(PPh_2)($CO)_3$(bpy)].

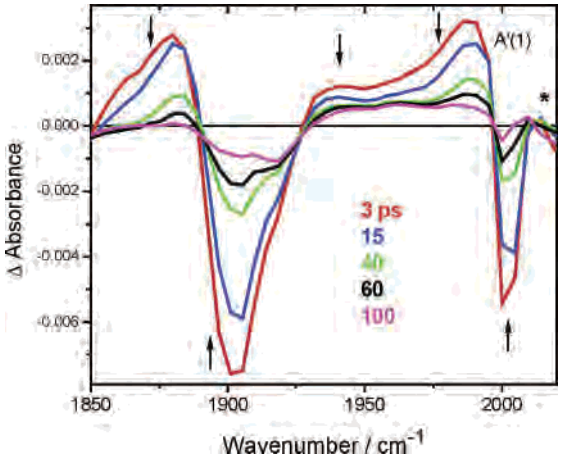

Figure 6. Difference TRIR spectra of [Re(PPh_2)($CO)_3$(bpy)] in THF measured at selected time delays (in ps) after 400 nm excitation. Experimental points are separated by 4−5 cm^{-1}. The spectrum evolves in the direction of the arrows. Spectra were recorded only at five time delays in order to shorten the measurement time and avoid sample decomposition. The asterisk denotes an artifact due to uncompensated solvent absorption.

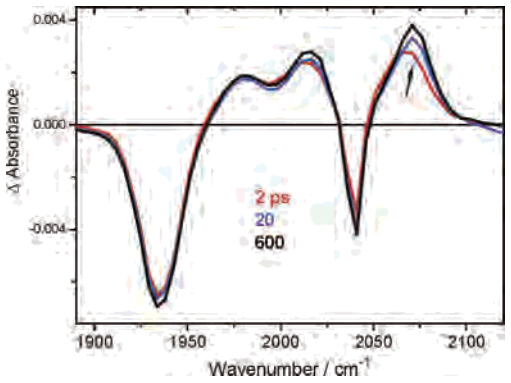

Figure 7. Difference TRIR spectra of [Re($NHPh_2$)($CO)_3$(bpy)]$^+$ in CH_3-CN measured at selected time delays (in ps) after 400 nm excitation. Experimental points are separated by 4−5 cm^{-1}. The spectral evolution in the direction of the arrows is caused by vibrational and solvent relaxation. Ground-state ν(CO) wavenumbers: 2041, 1934 cm^{-1}. Excited-state ν(CO) wavenumbers: 2071, 2017, 1981 cm^{-1}.

For comparison, we have measured TRIR spectra of [Re($NHPh_2$)($CO)_3$(bpy)]$^+$ and [Re(PPh_3)($CO)_3$(bpy)]$^+$, which are shown in Figures 7 and 8, respectively. The excited-state ν(CO) spectral patterns are very different from those of the amides and phosphides. The excited-state ν(CO) bands are shifted upward from their respective ground-state positions. In particular, a shift of +30 and +18 cm^{-1} was determined for the $NHPh_2$ and PPh_3 complexes, respectively. These

(28) Liard, D. J.; Busby, M.; Matousek, P.; Towrie, M.; Vlček, A., Jr. *J. Phys. Chem. A* **2004**, *108*, 2363−2369.
(29) Asbury, J. B.; Wang, Y.; Lian, T. *Bull. Chem. Soc. Jpn.* **2002**, *75*, 973−983.

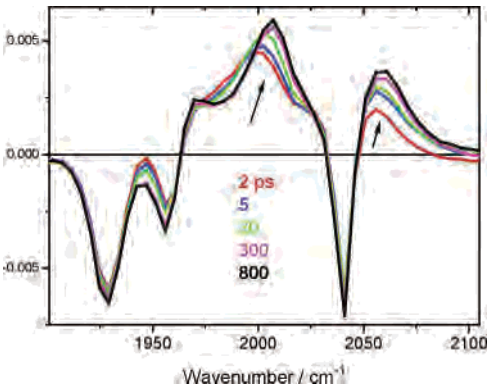

Figure 8. Difference TRIR spectra of $[Re(PPh_3)(CO)_3(bpy)]^+$ in CH_2Cl_2 measured at selected time delays (in ps) after 400 nm excitation. Experimental points are separated by 4−5 cm^{-1}. The spectral evolution in the direction of the arrows is caused by vibrational and solvent relaxation. Ground/excited-state ν(CO) wavenumbers: 2041/2059, 1957/2007, 1928/1965−1970 cm^{-1}.

upward shifts are typical manifestations of the Re → bpy MLCT character of their lowest excited states.[10,28,30−34] The smaller magnitude of the shift and rather unusual intensity pattern seen for the PPh_3 complex probably arise from through-space interaction between phosphine phenyl rings and the bpy ligand,[35] which may introduce some PPh_3 → bpy LLCT character into the excited state. The small dynamical upshift of the A′(1) band of both complexes, its narrowing, and increase in intensity are caused by the usual vibrational relaxation and solvent reorganization.[28]

DFT Modeling of the Lowest Triplet States. The lowest vertical triplet excitation energies of $[Re(NTol_2)(CO)_3(bpy)]$ and $[Re(PPh_2)(CO)_3(bpy)]$ were calculated by TD-DFT in THF as 1.36 and 1.82 eV, respectively. A value of 1.37 eV was obtained for $[Re(NHTol)(CO)_3(bpy)]$ in MeCN. The lowest triplet state results from 99% HOMO → LUMO excitation. A dense manifold of higher triplet states, which originate in a mixture of one-electron excitations, follows ca. 1 eV higher in energy, Tables S3−5.

UKS calculations were employed to optimize the structures and model the lowest relaxed triplet states. The 0−0 triplet energies of 1.17, 1.08, and 1.27 eV were obtained for the $NTol_2$, NHTol, and PPh_2 complexes, respectively. Emission energies were calculated much lower, 0.87, 0.86, and 0.54 eV, respectively, in accordance with the lack of any observable emission. The ground- and excited-state IR spectra of the amido complexes are well reproduced by calculations, Table 5. Excited-state bands were calculated to be only slightly shifted from their ground-state positions,

(30) Dattelbaum, D. M.; Omberg, K. M.; Hay, P. J.; Gebhart, N. L.; Martin, R. L.; Schoonover, J. R.; Meyer, T. J. *J. Phys. Chem. A* **2004**, *108*, 3527−3536.
(31) Dattelbaum, D. M.; Omberg, K. M.; Schoonover, J. R.; Martin, R. L.; Meyer, T. J. *Inorg. Chem.* **2002**, *41*, 6071−6079.
(32) Dattelbaum, D. M.; Martin, R. L.; Schoonover, J. R.; Meyer, T. J. *J. Phys. Chem. A* **2004**, *108*, 3518−3526.
(33) Gamelin, D. R.; George, M. W.; Glyn, P.; Grevels, F.-W.; Johnson, F. P. A.; Klotzbücher, W.; Morrison, S. L.; Russell, G.; Schaffner, K.; Turner, J. J. *Inorg. Chem.* **1994**, *33*, 3246−3250.
(34) George, M. W.; Johnson, F. P. A.; Westwell, J. R.; Hodges, P. M.; Turner, J. J. *J. Chem. Soc., Dalton Trans.* **1993**, 2977−2979.
(35) Tsubaki, H.; Tohyama, S.; Koike, K.; Saitoh, H.; Ishitani, O. *Dalton Trans.* **2005**, 385−395.

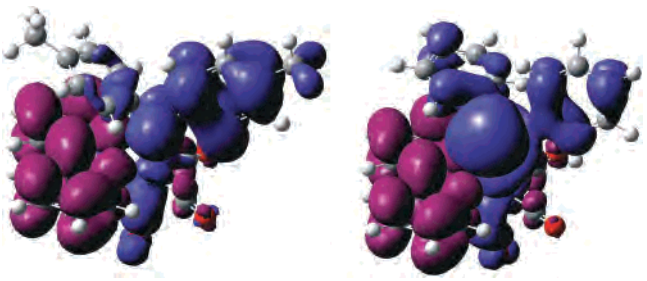

Figure 9. Electron-density difference between the lowest triplet state and the ground-state calculated by TD-DFT (PBE0/CPCM-THF) for $[Re(NTol_2)(CO)_3(bpy)]$ (left) and $[Re(PPh_2)(CO)_3(bpy)]$ (right) at the triplet geometry optimized by UKS. Blue and violet colors show regions of decreasing and increasing electron density upon excitation, respectively.

in agreement with experimental spectra, Figures 4 and 5. The higher A′(1) band was calculated to shift to lower wavenumbers by −8 and −4 cm^{-1} for $NTol_2$ and NHPh, respectively, in good agreement with the experimental shifts of ca. −6 and −4 cm^{-1}. A less satisfactory agreement was obtained for $[Re(PPh_2)(CO)_3(bpy)]$, whose A′(1) vibration was calculated to shift by +15 cm^{-1} in the lowest excited state, regardless of the conformer (shown in Figure S2) and basis set used for the phosphorus atom. A shift of ca. −9 cm^{-1} was estimated experimentally, Figure 6 and Table 5.

Figure 9, left, shows the electron-density difference between the lowest triplet state of $[Re(NTol_2)(CO)_3(bpy)]$ and the ground state, calculated at the optimized triplet geometry. It can be clearly seen that the electron density is transferred predominantly from the amide nitrogen atom and the π-conjugated phenyl ring to the bpy ligand, in accordance with the LLCT excited-state character. Much smaller electron depopulation occurs in the region of the Re atom and the axial CO ligand, while the electron density on the equatorial CO ligands slightly increases. LLCT character is also attributed to the lowest excited state of $[Re(PPh_2)(CO)_3(bpy)]$, see Figure 9, right. Here, most of the excited electron density originates in the lone electron pair on the phosphorus atom. The electron-density depletion around Re was calculated to be larger than for the amide.

The LLCT character of the lowest triplet state is also demonstrated (Table S7) by calculated differences of Mulliken populations between the lowest triplet and the ground state, calculated at their respective optimized structures. It follows that population of the lowest relaxed triplet state involves transfer of 0.65 or 0.54 e^- from an amido or phosphido ligand, while the charge on bpy increases by about 0.7 e^-. Population changes on Re and the CO ligands are much smaller.

Structural changes between the lowest ^{3}LLCT and the ground state of $[Re(NTol_2)(CO)_3(bpy)]$ and $[Re(PPh_2)(CO)_3(bpy)]$ are summarized in Table S8. In both complexes, the Re−N(bpy) bonds elongate on going to the excited state, presumably due to diminishing the Re → bpy π back-donation upon population of the π*(bpy) LUMO, i.e., reduction of the bpy ligand. The Re−N(amide) bond lengthens by 0.064 Å, possibly because of diminishing the amide basicity. The N donor atom maintains its planar sp^2

configuration upon excitation. The asymmetry between the two N−C(Ph) bonds increases due to strengthening the N−C(Ph) π interaction with the conjugated aryl ring upon depopulation of the HOMO, which is N−C(Ph) π-antibonding. The situation is somewhat different for the phosphide, where the Re−P and both P−C bonds were calculated to shorten on going to the excited state. At the same time, the geometry around the P atom "opens" toward planarity, as is manifested by the +45.7° change of the tilt angle between the RePC21 and RePC22 planes, from 110.5° to 156.2°. It follows that the ^{3}LLCT state of both complexes can be qualitatively viewed as $^3[Re(ER_2^{\bullet+})(CO)_3(bpy^{\bullet-})]$, containing an oxidized amide/phosphide radical-cationic ligand with an approximately planar sp^2 configuration of the N/P donor atom.

Discussion

The $[Re(ER_2)(CO)_3(bpy)]$ complexes studied herein are rare examples of molecules with an amido or phosphido ligand ER_2 bound to a low-valent, electron-rich metal atom. DFT calculations well reproduce the main structural features of these molecules, namely the planar and pyramidal configurations around the amido/phosphido N and P atoms, respectively. The HOMO of $[Re(NTol_2)(CO)_3(bpy)]$ (Figure 2) clearly shows that π-conjugation exists between the amido N atom and one aryl ring. On the other hand, no π-conjugation occurs between the P atom and any of the phenyl rings of the PPh_2 ligand in $[Re(PPh_2)(CO)_3(bpy)]$, whose HOMO looks like a phosphorus lone electron pair. Importantly, neither of the high-lying occupied MOs (Figure 2) of the amido complexes shows any π interaction between the amido N donor atom and Re dπ orbitals. The HOMO is the only high-lying MO with a large N contribution, which, however, is not matched by any significant Re dπ participation. The situation is similar for PPh_2. The presence of an amide/phosphide ligand-localized HOMO is a unique feature of the electronic structure of these complexes. Notably, it lies at relatively high energy, being well separated from the dense manifold of lower-lying occupied MOs, which contain contributions from the Re dπ and C≡O π* orbitals, as well as from amido/phosphido aryl rings, but not from the N/P donor atom. It follows that amides and phosphides are bound to Re(I) by a σ bond only, in accordance with the free rotation observed[1] by NMR at −80 °C. The absence of the Re−N/P π interaction clearly distinguishes the electronic structure of the amido/phosphido complexes from that of similar complexes $[Re(L)(CO)_3(bpy)]$ (L = halides, NCS^-), whose closely spaced HOMO and HOMO−1 are Re−L π-antibonding orbitals, while the corresponding pair of Re−L π-bonding orbitals lie at slightly lower energies.[8,10,27,30]

The presence of the high-lying, amido/phosphido-localized HOMO changes the spectroscopic and photophysical properties of the $[Re(ER_2)(CO)_3(bpy)]$ complexes relative to other Re(I) carbonyl−diimines. Generally, the lowest absorption band of the complexes $[Re(L)(CO)_3(bpy)]^{n+}$ (L = halides, NCS, pyridine derivatives, etc.) occurs slightly below 400 nm and, in most cases, originates in a transfer of electron density from the Re−L π-antibonding orbital (usually HOMO−1) to the π*(bpy) LUMO.[7,8,27,30,32,36,37] The lowest excited state then has a mixed Re → bpy MLCT/L → bpy LLCT character, the LLCT contribution increasing with the electron-donating ability of the ligand L. Because of the Re−L delocalized origin of excitation, it is more appropriate to call these excited states MLLCT (metal−ligand-to-ligand charge transfer).[8] The lowest excited state is usually closely followed in energy by a dense manifold of higher MLLCT and intraligand (bpy) states. The situation is profoundly different in the case of the amido/phosphido complexes. Here, the lowest electronic transition and the lowest triplet state are well separated from all other excited states, which occur more than 1 eV higher in energy. The lowest excited states of the amido/phosphido complexes originate in HOMO → LUMO excitation, having thus almost pure ER_2 → bpy LLCT character. The amido/phosphido ligand is depopulated by some 0.8 e^- in the optically prepared singlet and 0.6 e^- in the relaxed triplet, while the electron density at bpy increases by about 0.9 and 0.8 e^-, respectively, Tables S6, S7. Electron density on the $Re(CO)_3$ moiety changes much less. The excited electron-density originates predominantly in the π-delocalized N-aryl moiety for the amido ligands or the phosphorus lone electron pair of the PPh_2 ligand, which in the excited state attains a nearly planar, sp^2 geometry around the P atom. Because of the absence of any Re−ER_2 π interaction in the spectroscopically relevant MOs, the LLCT state does not contain any significant Re → bpy MLCT admixture. Such a "pure" LLCT excited state is unprecedented in the family of d^6 metal carbonyl−diimine complexes,[7,8] being entirely different from the MLLCT states seen, for example, for halide Re(I) complexes.

The ^{3}LLCT state is populated on a femtosecond time scale by intersystem crossing from the optically excited LLCT and LLCT/MLCT singlet states, which lie more than 16 000 cm^{-1} higher in energy. This energy excess is quickly dissipated into the internal and solvent vibrational modes. The ^{3}LLCT state is therefore initially formed "hot", that is, with nonequilibrated structure and solvation. Population of higher vibrational levels (mostly $v = 1$) of the ν(CO) A′(1) mode in the ^{3}LLCT state is seen for the amido complexes during the first few picoseconds after excitation. Cooling of the excited state, which includes vibrational energy redistribution (IVR) from higher ν(CO) vibrational levels, energy dissipation from low-lying vibrational modes into the solvent bath, and relaxation of the solvent shell to adjust to the new charge distribution in excited solute molecules, is clearly manifested (Figures 4 and 5) by the presence of the fast-decaying shoulder on the low-energy side of the A′(1) band, dynamical upward shift of the ν(CO) bands, and a pronounced dependence of the decay lifetime on the probe wavenumber. Relaxation processes follow multiexponential picosecond kinetics. The slowest relaxation step occurs with a time constant of 30−40 ps, that is, slower than vibrational cooling and solvent relaxation seen for analogous Re complexes in aprotic solvents.[28,29,37−39] Hence, it appears that relaxation

(36) Martin, R. L. *J. Chem. Phys.* **2003**, *118*, 4775−4777.

of excited amido complexes also involves intramolecular structural (conformational) changes. Only small signs of relaxation dynamics are seen in the TRIR spectra of [Re(PPh$_2$)(CO)$_3$(bpy)], possibly being obscured by fast excited-state decay.

The extensive structural reorganization in the lowest triplet LLCT state and solvent relaxation slightly diminish the charge separation between the ER$_2$ and bpy ligands in the lowest triplet state relative to the corresponding singlet (Tables S6 and S7). Moreover, the large distortion and very low excited-state energies decrease the lifetime of the lowest ^{3}LLCT state according to the energy-gap law. The lowest triplet state of the NTol$_2$ and NHTol complexes decay about 150−500 times faster than that of [Re(Cl)(CO)$_3$(bpy)]. The excited-state lifetime of [Re(PPh$_2$)(CO)$_3$(bpy)] is even shorter.

As far as the computational methodology is concerned, this work has again demonstrated that TD-DFT is able to calculate with good precision even those electronic transitions which involve a long-range interligand charge transfer, provided that a hybrid functional is used and the solvent is included.[8,27,40] The overall UV−vis spectral patterns of the amido and phosphido complexes are well reproduced by such calculations, Figure 3. The lowest ^{1}LLCT transition, which is most problematic[8] for TD-DFT, is underestimated by only 0.18, 0.29, and 0.58 eV for PPh$_2$, NTol$_2$, and NHTol, respectively. While TD-DFT optimization of excited-state structures did not converge, UKS triplet calculations have provided rather reliable description of the relaxed lowest triplet states and a good match between the calculated and experimental excited-state IR spectra of the amido complexes. The worse correspondence obtained for PPh$_2$ could be caused by the energetic proximity of the lowest triplet and the ground state in the phosphido complex. The single-determinant UKS approach and neglect of spin−orbit coupling might not be adequate at such a situation.

It is interesting to note that the ER$_2$ → bpy ^{3}LLCT state can actually be viewed as ^{3}[Re^{I}(ER$_2^{\bullet+}$)(CO)$_3$(bpy$^{\bullet-}$)]. This is an excited-state version of a highly unusual class of compounds where an aminyl or phosphinyl radical-cation is coordinated to a transition metal center and where the spin density is predominantly located on the ligated nitrogen or phosphorus atom.[6] This observation and the apparent photostability of these complexes suggest that ground-state phosphinyl/aminyl radical complexes of Re(I) could be generated by photochemical, chemical, or electrochemical oxidation of the [Re(ER$_2$)(CO)$_3$(bpy)] complexes. There is, to the authors knowledge, only one example of an isolated aminyl radical complex where the spin is located predominantly on the aminyl nitrogen.[6] A phosphorus analogue is yet to be discovered.

Conclusions

Amides and phosphides ER$_2$ (=NTol$_2$, NHTol, PPh$_2$) are electron-rich ligands which behave toward the Re^{I} atom in the complexes [Re(ER$_2$)(CO)$_3$(bpy)] as simple σ-donors. There is no π interaction between the N donor atom and Re dπ orbitals, while a very limited interaction is indicated for PPh$_2$.

The presence of a relatively isolated, ER$_2$-localized HOMO makes the spectroscopic properties, excited-state character, and dynamics of [Re(ER$_2$)(CO)$_3$(bpy)] profoundly different from other Re(I) carbonyl−diimine complexes. The lowest allowed electronic transition occurs at relatively low energies, being manifested by an isolated weak absorption band. It corresponds to essentially pure ER$_2$ → bpy ^{1}LLCT transition, the electron density distribution on the Re(CO)$_3$ moiety being affected only very little.

Optical excitation of [Re(ER$_2$)(CO)$_3$(bpy)] complexes is followed by intersystem crossing to a triplet state, whose structural and solvent relaxation occur with dynamics ranging from units to a few tenths of picoseconds. The lowest excited state is essentially pure ER$_2$ → bpy ^{3}LLCT. It can be qualitatively formulated as containing a coordinated aminyl/phosphinyl radical cation: ^{3}[Re(ER$_2^{\bullet+}$)(CO)$_3$(bpy$^{\bullet-}$)]. The large excited-state structural distortion and low energy provide for fast nonradiative decay to the ground state, making the ^{3}LLCT states very short-lived; 80−300 ps for the amides and about 30 ps for the phosphide.

Acknowledgment. Funding and support from the COST Action D35, CCLRC Rutherford Appleton Laboratory, QMUL and the Ministry of Education of the Czech Republic (Grant No. 1P05OC68) are gratefully acknowledged. The authors at Oviedo thank Professor Victor Riera and MCT (Grant No. BQU2003-08649) for support.

Supporting Information Available: DFT calculated data. This material is available free of charge via the Internet at http://pubs.acs.org.

IC0614768

(37) Busby, M.; Matousek, P.; Towrie, M.; Clark, I. P.; Motevalli, M.; Hartl, F.; Vlček, A., Jr. *Inorg. Chem.* **2004**, *43*, 4523−4530.
(38) Busby, M.; Matousek, P.; Towrie, M.; Di Bilio, A. J.; Gray, H. B.; Vlček, A. J. *Inorg. Chem.* **2004**, *43*, 4994−5002.
(39) Blanco-Rodríguez, A. M.; Busby, M.; Grădinaru, C.; Crane, B. R.; Di Bilio, A. J.; Matousek, P.; Towrie, M.; Leigh, B. S.; Richards, J. H.; Vlček, A., Jr.; Gray, H. B. *J. Am. Chem. Soc.* **2006**, *128*, 4365−4370.
(40) Gabrielsson, A.; Matousek, P.; Towrie, M.; Hartl, F.; Záliš, S.; Vlček, A., Jr. *J. Phys. Chem. A* **2005**, *109*, 6147−6153.